Astronomy
&
Astrophysics

BeppoSAX broad X-ray range observations of η Carinae during high and low spectroscopic states[⋆]

R. F. Viotti[1], L. A. Antonelli[2], M. F. Corcoran[3], A. Damineli[4], P. Grandi[1], J. M. Muller[5], S. Rebecchi[6], C. Rossi[7], and M. Villada[8]

[1] Istituto di Astrofisica Spaziale e Fisica Cosmica, CNR, Area di Ricerca Tor Vergata,
Via Fosso del Cavaliere 100, 00133 Roma, Italy

[2] INAF-Osservatorio Astronomico di Roma, Via Frascati 33, 00040 Monte Porzio Catone (Roma), Italy

[3] Universities Space Research Association, 7501 Forbes Blvd, Ste 206, Seabrook, MD 20706, and Laboratory
for High Energy Astrophysics, Goddard Space Flight Center, Greenbelt MD 20771, USA

[4] Instituto Astronomico e Geofisico da Universidade de São Paulo, Av. Miguel Stefano 4200, 04301-904 São Paulo,
Brazil

[5] University Hospital Nijmegen, Department of Radiology, PO Box 9101, 6500 HB Nijmegen, The Netherlands

[6] ASI Science Data Center (ASDC), c/o ESA-ESRIN, Via Galileo Galilei, 00044 Frascati (Roma), Italy

[7] Dipartimento di Fisica, Università La Sapienza, Piazzale Aldo Moro 3, 00185 Roma, Italy

[8] Dep. Astronomia Estelar, Observatorio Astronomico U.N.C., 5000 Cordoba, Argentina

Abstract. We present BeppoSAX spectra of the extremely luminous and massive object η Car observed in a very broad X–ray range (0.1–200 keV) during high state (December 1996) and egress from the last low state (March 1998). Both spectra are composed of at least two components, a soft one with $kT_s < 0.7$ keV, and a hard with $kT_h = 4.7$ keV. We found in March 1998 a large flux defect in the 1.5–4 keV range, while the flux remained constant below 1.5 keV and above 5 keV. We attribute this defect to a $\times 3.5$ increase of the absorbing matter in front of the hard component, while its temperature and unabsorbed luminosity were nearly the same in the two epochs. In December 1996 the PDS X–ray flux in the 13–20 keV range is larger than the extrapolated hard spectrum, indicating the presence of an even harder additional component, which possibly declined during the March 1998 low state. Conversely, we find that at that time, the flux of the 6.7 keV iron line was 40% stronger. Coordinated optical and NIR spectroscopic observations indicate that in March 1998 η Car was still in a state of low excitation of the emission line spectrum, with extended P Cygni absorptions. These results indicate that after the X–ray flux minimum, the hard component recovered its high state luminosity more rapidly than the high ionization spectral lines, but in the meantime it was partly occulted by a large amount of absorbing matter placed in front of the source. These results are discussed in the framework of the proposed binary model of η Car.

Key words. stars: binaries: spectroscopic – stars: emission-line, Be – stars: individual: η Car – stars: mass loss – X-rays: stars

1. The η Car problem

η Car is an outstanding object of the upper H–R Diagram that underwent dramatic light variations in the 19th cen-

---

tury, ejecting large quantities of matter now forming an extended nebula (the *homunculus*). The star is still losing matter at a high rate in the form of a high speed massive wind. The spectroscopic history of η Car is characterized by extended "high states", when the optical emission line spectrum is very prominent with a large range in ionization, and by occasional "spectroscopic events" (or "low states") characterized by a deep fading of the high excitation emission lines, typically lasting several months (e.g. Rodgers & Searle 1967; Viotti 1969; Zanella et al. 1984; Altamore et al. 1994). Recently, Damineli (1996) reported that the events repeat periodically every 5.53 y. These recurrent low–excitation events have been attributed by

Damineli et al. (1997) to binarity in agreement with the radial velocity curve of the Paγ 1.094 μm emission line. The binary model of η Car was later confirmed by Damineli et al. (2000), although their method of derivation of the orbital parameters has been questioned (e.g., Davidson et al. 2000). According to Damineli et al. (2000) the system would consist of a very massive primary ($\approx$70 $M_\odot$), which presently is the most luminous (S Doradus–type) component of the system, and an unseen early–type companion star whose nature is still unknown. The orbit should be very eccentric, resulting in a very close periastron passage (a few AU). In addition, both stars should have a massive stellar wind, and one would expect that the collision between the two winds would produce a hot plasma and generate high energy X–rays. A new low excitation event occurred near the end of 1997, which peaked in December 1997 (see Fig. 1). A world–wide campaign of multifrequency ground–based and space–borne observations was therefore organized and some results of which will be presented here. We shall adopt from Damineli et al. (2000) the following ephemeris for the spectroscopic minimum: Min = JD 2450794 (12 December 1997) + 2020 E.

The Carina region frequently has been observed in X–rays during the last two decades. The spatially resolved *Einstein Observatory* observations revealed that the emission is spatially structured, consisting of a point–like hard source (ηHX) coincident with the stellar core, and an inhomogeneous shell source (ηSX) surrounding the homunculus (Chlebowsky et al. 1984). Evidence for X–ray variability was first given by ROSAT. From PSPC observations obtained near the June 1992 spectroscopic minimum, Corcoran et al. (1995) found that the emission above 2 keV was extremely weak. Geometrically, the variation was confined to the hotter central point source ηHX. A new weakening (or "eclipse") of the hard X–ray source occurred at the time of the last spectroscopic low state of December 1997, and was investigated with ASCA (Corcoran et al. 2000), RossiXTE (Ishibashi et al. 1999; Corcoran et al. 2001), and BeppoSAX (Viotti et al. 1999).

In this paper we discuss the BeppoSAX observations made during egress from the last event, and compare them with the observations made with the same equipment during the previous high state. The observations and data reduction are discussed in Sect. 2. In Sect. 3 we describe the time variability of the X–ray energy distribution and of the 6.7 keV line, and derive the best fitting spectral parameters of the X–ray spectrum. We also discuss a selection of optical spectra taken during the long–term monitoring of the spectroscopic state of the object. The derived results are discussed in Sect. 4 in the light of the proposed binary model. Conclusions follow in Sect. 5.

2. Observations and data analysis

η Car was first observed by BeppoSAX on 29–30 December 1996, when the star was in a "high spectroscopic state" of its 5.53 y variability cycle ($\Phi = 0.828$). The observations covering a wide energy range have been obtained by
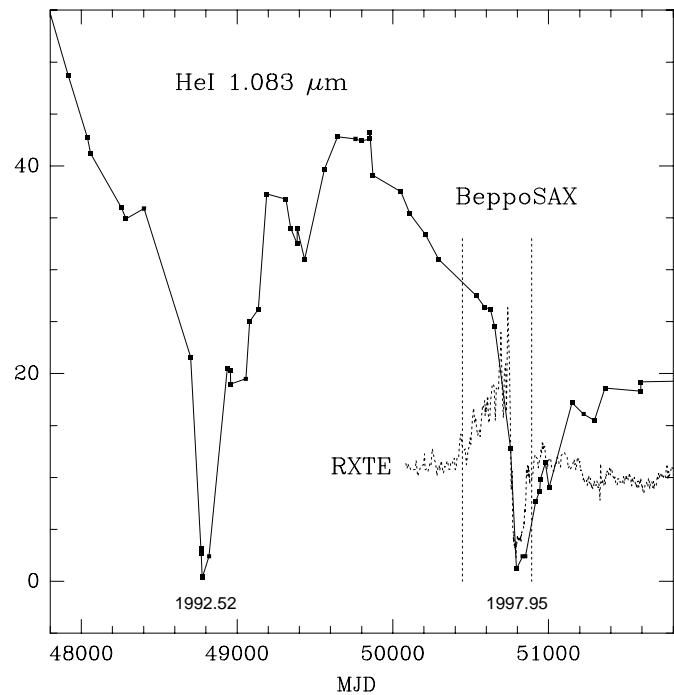

Fig. 1. The cyclic variation of the He I 1.083 μm emission line during 1990–2000 compared with the RossiXTE X-ray light curve. The epochs of the BeppoSAX observations (vertical bars), and of the last two spectroscopic minima of June 1992 and December 1997 are marked. Ordinates are emission line equivalent widths (in nm) and RossiXTE background subtracted countrates (s^{-1}).

the BeppoSAX instruments: LECS ($\sim$0.1–10 keV), MECS (1.3–10 keV), and PDS (13–200 keV), with η Car always placed at the centre of the field of view. PDS has no imaging capability, but η Car is the dominant source within the fields of view. Three MECS units were in operation at the time of this observation. Subsequently, η Car was observed again by BeppoSAX as a target–of–opportunity (TOO) during the international campaign organized on the occasion of the December 1997 event. The BeppoSAX observation was performed on 18–19 March 1998, at the spectroscopic phase $\Phi = 0.048$, again with LECS, MECS, and PDS, but with only two MECS units, MECS1 being not in operation. Details of the BeppoSAX observations are given in Table 1. The December 1996 LECS and MECS images of the η Car region are shown in Fig. 2.

As a completion of this research, high resolution optical spectra were collected on 27 March 1997, and 7 February and 14 April 1998 with the 1.6 m telescope of the Laboratório Nacional de Astrofísica (LNA/MCT, Brazil) and on 20–21 February and 21 December 1997, and 6 May 1998 with the 2.15 m telescope of the CASLEO Observatory (El Leoncito, Argentina).

Data preparation and linearization of the BeppoSAX observations was performed using the SAXDAS package. X–ray data analysis was made using FTOOLS and the XANADU S/W package. We have extracted for the LECS and MECS images all the events within a circular region

Table 1. Journal of BeppoSAX observations of η Car.

date	Julian Day JD-2 400 000	instrument	effective exp. time (10^3 s)	[energy range] (keV)	countrate[a] (s^{-1})	remarks
1996 Dec. 29–30	50447	LECS	17.4	[0.1–10.]	$0.071 \pm .002$	
($\Phi = 0.828$)		MECS123	46.3	[2.0–10.]	$1.108 \pm .005$	
		PDS	19.5	[13.–200.]	$0.15 \pm .05$	
1998 Mar. 18–19	50891	LECS	22.6	[0.1–10.]	$0.053 \pm .002$	
($\Phi = 0.048$)		MECS23	39.0	[2.0–10.]	$0.553 \pm .004^b$	
		PDS	16.4	[13.–200.]	<0.15	3σ upper limit

Notes to the table: [a] LECS and MECS countrates from a 4 arcmin radius extraction aperture. [b] Flux corrected for the different number of MECS detectors. [c] Phase of the 5.53 y cycle, according to Damineli et al. (2000).
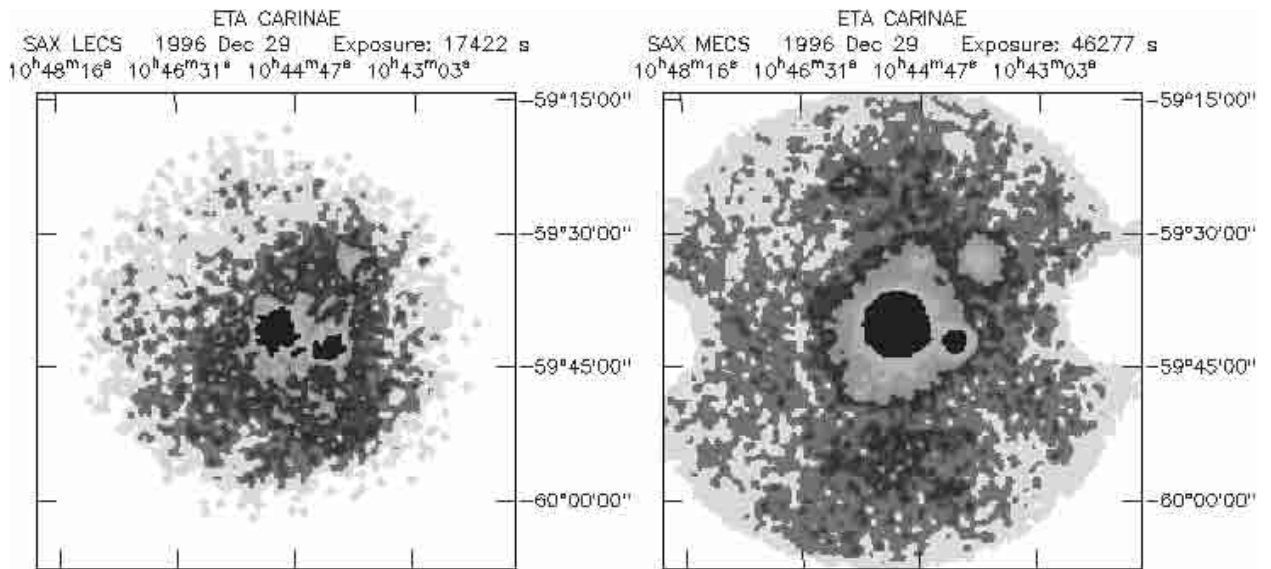

Fig. 2. The BeppoSAX LECS (0.1–2 keV, left) and MECS (2–10 keV, right) images of 1996 December 29–30 centred on η Car. North is to the top and east to the left. η Car is the strongest and hardest source in the field. Many other point sources are present in the field, including: HD 93250 (O5V, 7′ N), the WN6 star HD 93162 (6′ W), HD 93403 (O5IIf, 17′ N), and the Trumpler 14 association (10′ NW). The diffuse emission from the Carina nebula is visible in the LECS image.

of 4 arcmin radius centred on the emission peak of the η Car source. Data taken from the different MECS units were combined together. The size of the circle is such as to ensure the collection of 90% of the source events in the MECS images, and to exclude most of the events from the nearest X–ray sources. The X–ray emission from the O3V star HDE 303308, about 1 arcmin to the northeast of η Car, is not resolved by BeppoSAX, but previous Einstein and ROSAT observations indicate that the source is softer and much weaker than η Car. Hereafter, its contribution to the strong η Car source will be neglected. The LECS PSF is somewhat larger at 1.5 keV than the MECS one, and the spatial resolution degrades for energies much below 1 keV. Therefore, using a 4 arcmin extraction radius many source photons are lost in the low energy region of LECS. We have extracted background counts from different regions around η Car always using an extraction aperture of 4 arcmin radius. In the LECS images the background

varies irregularly from one place to another due to the variable nebular emission, which makes it difficult to estimate the contribution of the nebula to the source in this band, even using the small extraction aperture. For the background subtraction we finally selected a region at $\sim 10'$ SE of η Car. For the MECS spectra, we did not experience with similar problems as the source count rate is much higher than that of the nebular background. The nebular background–subtracted spectra of η Car in the two epochs are shown in Fig. 3. As already noted in the previous X–ray observations, the spectrum clearly appears (at least) bimodal, with low and high temperature components, which we shall refer to in the following as ηSX and ηHX, respectively. A prominent emission is present in both epochs near 6.7 keV due to the iron emission blend.

During the BeppoSAX observations the Carina region was also observed with the PDS detector. A significant countrate (0.147 ± 0.054 s^{-1}) was detected in
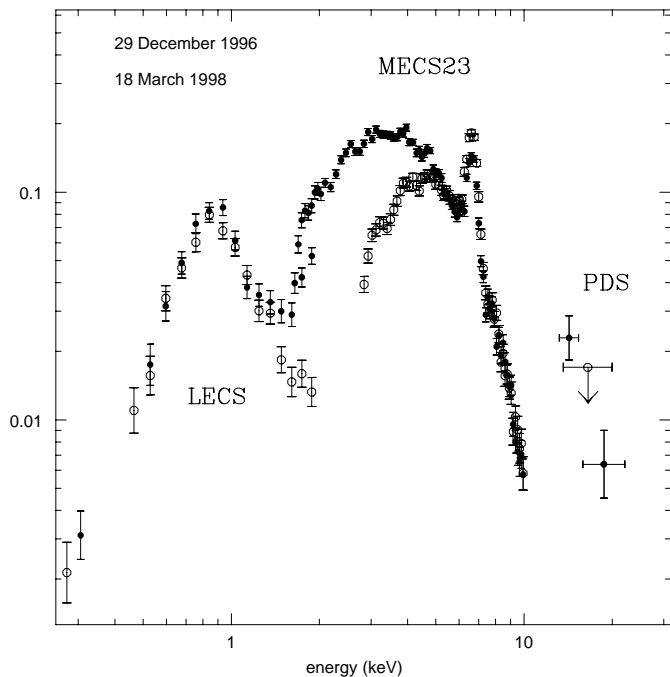
Fig. 3. The BeppoSax countrates (in s^{-1} keV^{-1}) of η Car during high (29–30 December 1996, *filled circles*), and low states (18–19 March 1998, *open circles*. Two MECS units are considered for the 1996 observations. The 1 σ error bars are also shown. Only a countrate upper limit (3σ) was set by the PDS detector in March 1998. Notice the enhancement of the 6.7 keV feature in March 1998.

Fig. 4. Ratio of BeppoSAX countrates of December 1996 and March 1998. Notice the large flux variation in the 1.5–4 keV range and the constancy outside this range. The inset illustrates with an enlarged vertical scale (right), the enhancement of the Fe-k emission feature in March 1998.

December 1996 in the 13–20 keV range with a steep negative spectral slope (Fig. 3). η Car being the strongest and hardest source in the MECS field, we can safely attribute all the PDS photons to this source. Actually, the PDS field of view also includes the pulsar 1E1048.1-5937, which could possibly contribute to the PDS countrate. However, using the published X–ray spectrum of this object (e.g., Osterbroek et al. 1998), it turns out that its flux near 10–20 keV is much fainter than that of η Car in December 1996. This is the first detection of η Car above 10 keV. For the March 1998 PDS observation we can derive only a 3 σ upper limit of 0.15 s^{-1}.

3. Results

3.1. Short and long term X–ray time variability

Before proceeding to the spectral analysis, we studied the time variability of the η Car source. We first compared the 1996 and 1998 BeppoSAX observations in order to demonstrate those changes that could be of help in making the following fits. As shown in Table 1 and Fig. 3, in the March 1998 observations the LECS and MECS count rates were significantly smaller. The flux variation in different energy bands is illustrated in Fig. 4 where we plotted the 1996/1998 count rate ratio in the LECS and MECS detectors as a function of energy. For uniformity, we took the
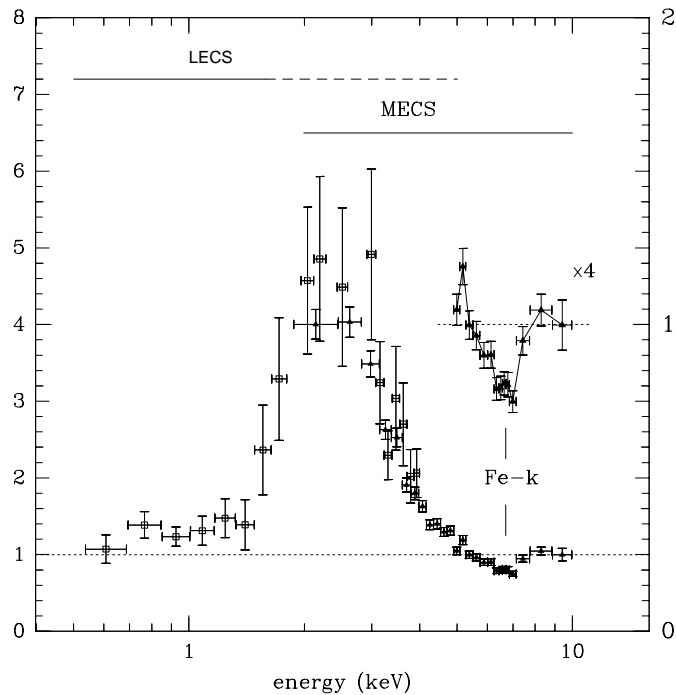
photons from two MECS units for both observations. The large decrease in the 1.5–4 keV range is evident in the figure with a maximum factor of 4–5 near 2–3 keV, while the flux was nearly the same below 1.5 keV and above 5 keV. The width and shape of the 1996/1998 flux ratio clearly indicate that the variation has to be attributed essentially to a large increase of the absorption column density of the ηHX component, with a small or null variation of the unabsorbed hotter source, and with the soft component being steady. As illustrated in Fig. 3, and more clearly in Fig. 4, the flux of the 6.7 keV line is significantly larger ($+40 \pm 10\%$) during the low state observations of March 1998, in contrast with the constancy of the underlying continuum. This point and its model implication will be discussed in details below in Sect. 4.

We have also looked at the short time variability for the individual LECS and MECS observations in different energy bands, using different binning times (from 1500 to 5700 s, the latter one corresponding to the satellite orbital period). We have found no significant evidence for short–term periodic variation for both epochs. However, we noted that the countrate irregularly fluctuates with an amplitude which sometimes exceeds 3σ, with no correlation between different bands. We also found for the March 1998 4.5–10 keV band a marginal indication of a flux decrease during the 22 hours of BeppoSAX observations, while the intermediate band flux is consistent with a constant flux.

Table 2. Best fit spectral parameters of BeppoSAX observations.

JD$-2\,400\,000$ best fit	50447 2-comp	50447 brems+gauss	50891 2-comp	50891 brems+gauss
ηSX *component*:				
kT_s (keV)	$0.13 \pm .02$		$0.75 \pm .07$	
$NH_s/10^{22}$ cm^{-2}	$0.89 \pm .15$		$0.16 \pm .04$	
$[N/H]$ [a]	$0.23 \pm .28$		$1.96 \pm .18$	
ηHX *component*:				
kT_h (keV)	$4.78 \pm .10$	$5.16 \pm .18$	$4.35 \pm .15$	$4.76 \pm .20$
$NH_h/10^{22}$ cm^{-2}	$4.33 \pm .08$	$4.33 \pm .14$	$15.4 \pm .4$	$15.2 \pm .4$
$f_x[2\text{-}10]$ [b]	$7.33 \pm .03$	7.28	$6.12 \pm .04$	6.05
$f_x^o[2\text{-}10]$ [c]	9.41	9.35	12.7	12.6
Fe-k W_{eq} (keV)	$1.09 \pm .06$	$1.01 \pm .06$	$1.32 \pm .09$	$1.41 \pm .09$
Fe-k E_{peak} (keV)		$6.735 \pm .007$		$6.724 \pm .008$
Fe-k $FWHM$ (keV)		≤ 0.1		$0.28 \pm .05$
$[Fe/H]$[a]	$-0.12 \pm .01$		$-0.01 \pm .13$	
reduced χ^2	2.57	1.95	2.08	1.36

Notes to the table: [a] Logarithmic abundance ratio referred to the solar abundance derived from the MEKAL fit. [b] Observed 2–10 keV X-ray flux, in 10^{-11} erg cm^{-2} s^{-1}. [c] Unabsorbed 2–10 keV flux, in 10^{-11} erg cm^{-2} s^{-1}.

3.2. The X–ray spectrum

3.2.1. Two–component fitting

The LECS, MECS and PDS background–subtracted spectra were fitted using the MEKAL thermal collisional–equilibrium models which allow a two–component fitting and, if required, to adjust the chemical composition. The final fitting parameters are given in Table 2. We have first analysed the March 1998 LECS+MECS spectrum where the two components are better separated and used the ASCA results from Tsuboi et al. (1997) and Corcoran et al. (1998) as guess parameters. The best fit of the spectrum with a two–component model with solar abundance gives for the hard component quite a large absorption column density of about 1.5×10^{23} cm^{-2}, in agreement with the 4 keV cutoff shown in Fig. 3, while the temperature kT_h (4.4 keV) is consistent with the previous ASCA estimates. The best fit has a rather high reduced χ^2 value of 2.94, the largest contribution to the residuals coming from energies below 0.9 keV and around the 6.7 keV line. If we allow the nitrogen and iron abundances to vary, a large nitrogen overabundance is found, in agreement with the ASCA results, with an improved reduced χ^2 of 2.08. The soft component temperature, however, results unrealistically high ($kT_s = 0.75$ keV) well probably because of the distorsion of the spectrum due to the difficult background subtraction discussed in Sect. 2. The iron abundance turns out to be solar, while no significant deviation from the cosmic abundance is found for the other elements, which were therefore put equal to solar in the fitting procedure. However, there are significant residuals

near the iron line, with a negative peak near 6.5 keV and an excess peaking at 6.9 keV. This wave–type shape is an indication that the actual peak of the line is centred to an energy higher than that expected ($\sim$6.69 keV) for the derived temperature of the hard component.

We have applied the same procedure to the December 1996 LECS and MECS spectrum, using the March 1998 parameters as an initial guess for the best fit. In this case a more realistic value for kT_s is derived, but at the cost of a nearly normal nitrogen abundance. The hard component resulted in a temperature slightly higher than that derived for March 1998, while the absorption column density is much lower (4.3×10^{22} cm^{-2}) in agreement with the previous ASCA high state observations. The iron abundance is slightly lower than solar, but the best fitting procedure leaves out negative and positive residuals similar to those observed in the March 1998 spectrum. As for the PDS spectrum, no model of the hard component could adequately fit the flux above 10 keV, leaving out a 2σ excess at 13–15 keV. The low countrate prevents the fitting of this hard X–ray tail with an additional component, but we may argue that if thermal emission, it should originate from a hotter region that is more compact than that of ηHX.

3.2.2. Bremsstrahlung plus the 6.7 keV line fitting

In order to better investigate the spectrum of η Car near the iron feature and to improve the best fit, we have adopted a simple model combining a pure bremsstrahlung spectrum with photoelectric absorption, and a Gaussian
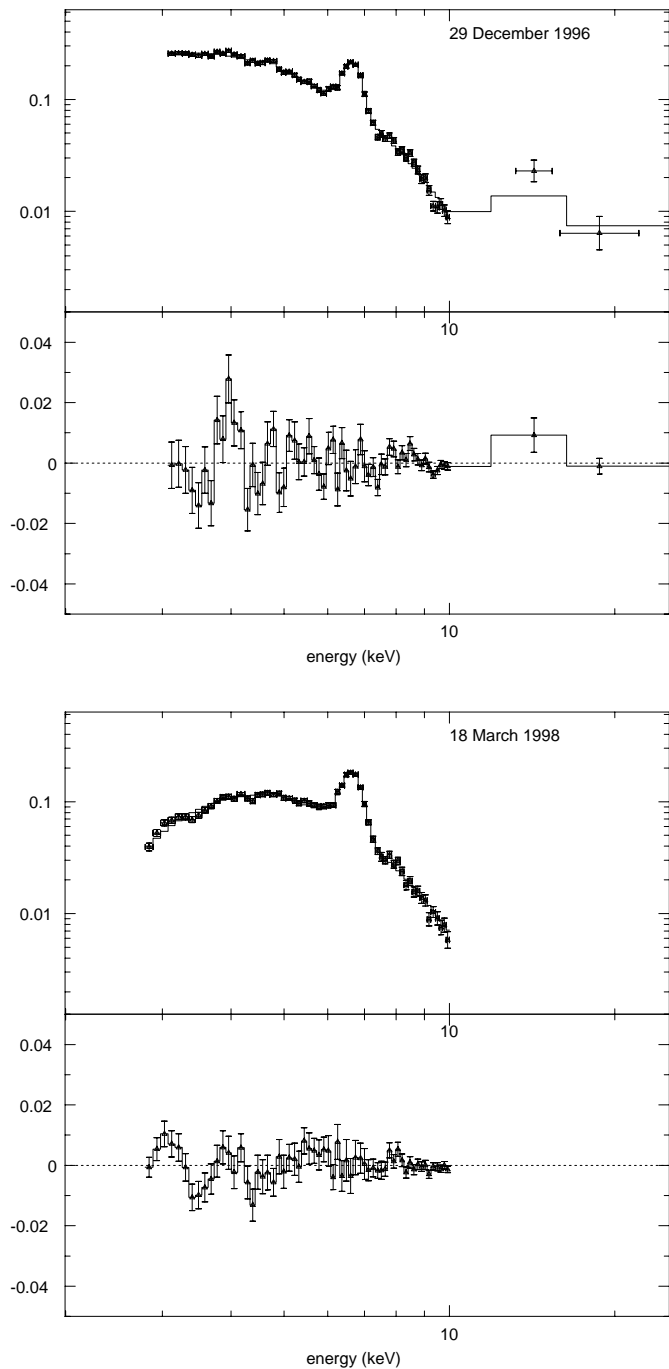
Fig. 5. The BeppoSAX MECS countrates of η Car fitted with a thermal bremsstrahlung plus a Gaussian line model. The lower panels give the residuals in an expanded linear scale. The PDS observations are also included in the upper panel.

profile near the 6.7 keV line. The line strength and width, and the peak energy are free parameters. We have also selected the MECS countrates above 3 keV in order to reduce to a minimum the effects of the soft X–ray component. For December 1996 the PDS data are also included in the fit. The best fit parameters are given in Table 2, and the observed spectra fitted with the bremsstrahlung plus Gaussian line model are shown in Fig. 5. We first note that the temperatures ($kT_{\rm h}$) are slightly larger with respect to

the two–component fit, but the absorption column densities $NH_{\rm h}$ are the same. In addition, the fit of the December 1996 spectrum leaves again a 2 σ flux excess near 13–15 keV. The best fit width of the 6.7 feature in December 1996 is consistent with an unresolved line, while in March 1998 it is consistent with a broad line having a *FWHM* of $0.28 \pm .05$ keV. In both epochs the line is unexpectedly centred at 6.73 keV. In fact, the theoretical computations of e.g. Mewe et al. (1985) show that at a temperature $kT_{\rm h} \leq 5$ keV the main emission components to the iron feature are the transitions of the helium–like Fe XXV at 6.64 keV, 6.68 and 6.70 keV, with a negligible contribution of the hydrogen–like Fe XXVI 6.97 keV line. In addition, the blend should also include the iron fluorescence line at 6.4 keV, that was resolved from the main component in the ASCA X–ray spectra of η Car (Corcoran et al. 1998, 2000). We therefore expect the 4.7 keV plasma to produce an iron line centred at $\sim$6.69 keV. The observed line shift to a larger energy would imply a significant contribution of the 6.97 keV emission line, and line formation in a plasma with a temperature (about 6.3 keV) much higher than that of the continuum. However, after the completion of this research we were informed of a possible small miscalibration of the energy pulse height–channel relationship near the iron line, amounting to about +40 eV near the iron line (e.g. Molendi et al. 2000). Since the shift of the line centroid in the spectra of η Car with respect to the expected energy has the same value ($+40 \pm 5$ eV), we argue that this effect could be an instrumental artifact. We finally have tried to also include in the fit a second Gaussian line centred at the energy of the fluorescence iron line, but the spectral analysis did not give a positive result.

3.3. Spectroscopic observations

Figures 6 and 7 illustrate some of the optical observations collected on the occasion of the BeppoSAX observations, although not simultaneously. Figure 6 shows the high resolution near–infrared spectra of η Car taken during 1997–98 with the Brazilian LNA telescope. In March 1997 the He I 1083 nm metastable line displayed a very intense emission line with a narrow peak doubled by a central absorption. The line also presented two absorption components centred at -500 and -1050 km s^{-1}, respectively. These two components were already present during the previous 1990–1991 observations of Damineli Neto et al. (1993). In February 1998 the helium emission line largely faded, leaving only a weak emission with a broad red tail, and a narrow central absorption. The lower velocity P Cygni absorption had largely strengthened and broadened, and extends to -600 km s^{-1}. The strengthening may be at least partly explained by the weakening of the emission line component. At that time, the narrow peak of Pγ was absent, as well as the weak Fe II emission line at 1086 nm was (Fig. 6). These lines reappeared in April 1998, at which date the He I emission line started to brighten again,
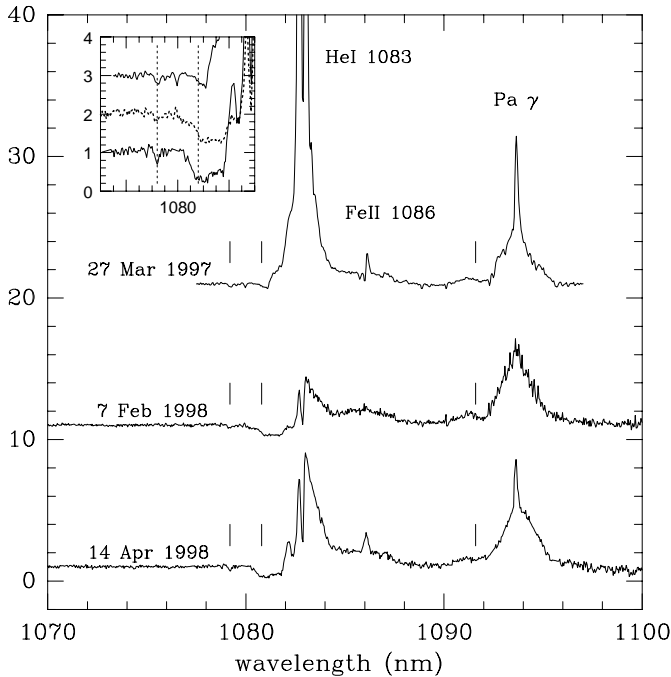
Fig. 6. The NIR spectrum of η Car during high and low states (LNA Observatory). Vertical bars mark the He I P Cygni absorption components at -600 and -1050 km s^{-1}, and the -600 km s^{-1} components of Pγ. Ordinates are fluxes normalized to continuum. Successive spectra are offset by 10 continuum units. The P Cygni absorptions of He I are shown enlarged in the inset.

Fig. 7. Spectral variation of η Car during 1997–1998 (CASLEO Observatory). The vertical bars mark -600 km s^{-1} in the P Cygni absorption profile of H8. Fluxes are normalized to continuum, with 2 continuum units' offsets for successive spectra.

while the broad P Cygni absorption remained nearly unchanged.

The CASLEO optical spectra of η Car near the high excitation [Ne III] emission line are shown in Fig. 7. In February 1997, two months after the earlier BeppoSAX observations, the high excitation [Ne III] 386.874 nm line was present with a strong emission, but the line completely disappeared in December 1997 at the time of the spectroscopic event, and was still absent in May 1998, two months after the second BeppoSAX observations. A behaviour similar to that of [Ne III] was observed in the CASLEO spectra by the [Fe III] and He I emission lines near 501 nm, and by the prominent [N II] yellow emission line. We finally remark some weakening of the H I and Fe II emission lines during the spectroscopic event (see Figs. 6 and 7). McGregor et al. (1999) also reports the dramatic decrease in December 1997 of the high excitation emission lines and of the narrow components of H I and of Fe II, and the appearence of prominent blue shifted absorptions in the hydrogen Balmer and Paschen lines.

The ultraviolet spectrum of η Car was monitored at regular intervals with the International Ultraviolet Explorer (IUE) from December 1992 until July 1996. During this period the trend of the UV emission lines (e.g., Si III], C III], Fe III) well matches that of He I 1083 nm, with a flux maximum in mid 1995, followed by a slight flux decrease in July 1996 (Viotti et al. 1998), four months before the first BeppoSAX observations. We should also
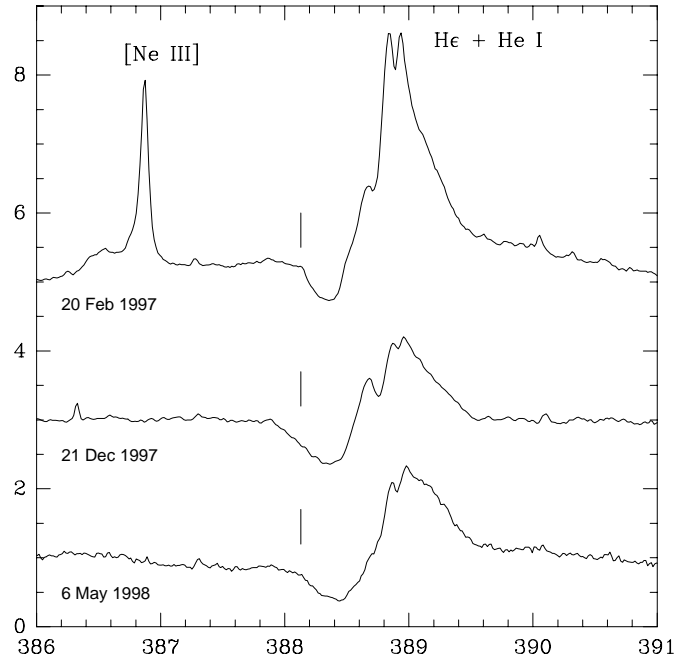
notice that the optical–ultraviolet spectrum of η Car was observed with the STIS spectrograph onboard the Hubble Space Telescope on 19 March 1998, at the same time as the second BeppoSAX observations. As shown by Davidson et al. (1999) at that date the spectrum was marked by a flux defect in the UV due to the large line absorption (mostly of Fe II), and the strengthening of the P Cygni absorptions in the visual, similar to that observed by us at LNA and CASLEO.

4. Discussion

4.1. The high and low states of η Car

According to the spectroscopic monitoring, at the time of the first BeppoSAX observations of December 1996 η Car was in a phase of gradual fading of the optical and UV emission lines, following the spectroscopic maximum of 1995, probably the result of the weakening of the source of UV radiation, which, in the proposed binary model, is provided by the unseen component (Damineli et al. 1997). As shown in Fig. 1, these BeppoSAX observations were made just before the beginning of the gradual increase of the X–ray flux recorded by RossiXTE (Ishibashi et al. 1999). This increase suddenly stopped at the end of November 1997 when the X–ray flux dropped to a very low value. The epoch of the X–ray minimum nearly coincides with the spectroscopic minimum (12 December 1997, according to Damineli et al. 2000).

The ASCA observations made on 24 December 1997 revealed that the X–ray flux in the 2–10 keV range was

about ten times weaker, which Corcoran et al. (2000) attributed to a large luminosity decline of the unabsorbed luminosity of the ηHX source. The X–ray low state ended in February 1998 when the RossiXTE flux began to rise. Since March–April 1998 the countrate remained around the same value as before 1997, though with large oscillations (or "flares"). Conversely, one may notice from Fig. 1, and from the spectrograms taken in April–May 1998 (Figs. 6 and 7), that the recovering of the emission line spectrum was slower than the X–ray one. A similar slow flux increase was also observed in the IR (Feast et al. 2001), and in the radio (White 2001).

The second BeppoSAX observations were made just after the first flux flare that followed the low state. We have found that the BeppoSAX 2–10 keV observed flux $f_x[2–10]$ was at that time $\sim 17\%$ lower than that of December 1996, in good agreement with the respective RossiXTE fluxes (Ishibashi et al. 1999). However, we have also found that the absorption column density in March 1998 was $\times 3.5$ larger than during high state. We recall that according to the ASCA (Corcoran et al. 2000), and RossiXTE observations (Ishibashi et al. 1999) the absorption column density NH_h was low at the time of the X–ray minimum of December 1997. From this result we must argue that between December 1997 and March 1998 an opaque region was interposed in the line of sight. This was also invoked by Ishibashi et al. (1999) to explain the long duration of the flat X–ray minimum and the asymmetry of the X–ray light curve. The presence of a region of enhanced density can be explained at least qualitatively in the light of theoretical models of the interaction region in colliding–wind binary systems. These models envisage as the result of the orbital motion, the formation of spiral shaped wind boundaries (e.g., Eichler & Usov 1993; Walder et al. 1999), that near periastron should be closer to the stars and denser. Alternatively, the absorbing region could be identified with a large sized equatorial disk surrounding the S Dor star, as invoked by Ishibashi et al. (1999), while Corcoran et al. (2001) suggest a considerable increase of the mass loss rate from η Car near periastron, possibly driven by tidal interactions.

4.2. The emitting region

At odds with the behaviour of the 5–10 keV continuum flux during the two BeppoSAX observations, the 6.7 keV emission line exhibited in March 1998 a significant flux (and equivalent width) maximum, as if the line would be at least partly arising in a region different from that where the continuum is formed. One may argue that this region is also responsible for the flux excess in the 13–20 keV region (the "hard X–ray tail") observed in December 1996 which, if thermal emission, would be produced by a hotter plasma. The possible decline of the hard tail in March 1998 in contrast with the flux increase of the 6.7 keV line, might appear not compatible with a common origin. However, we might at least tentatively consider that the more compact

hotter source could have been partly occulted near conjunction by the dense wind of the S Dor star, while its radiation is still heating a more extended unocculted iron region.

Let us now tackle another problem. As shown in Sect. 3.2, the thermal model fittings of the 2–10 keV BeppoSAX spectra provide an iron abundance equal to solar (in 1998), or slightly smaller than solar (in 1996). Similarly, the thermal modelling of the 1996 ASCA spectra gives [Fe/H] $= -0.12 \pm 0.01$ (Corcoran et al. 1998). But, if the iron line in order to account for its variability is at least partly formed elsewhere, the above derived abundances of the ηHX component should be taken as upper limits, the actual abundances could be significantly lower than solar. This could be not unexpected in the case of η Car, since it is known that dust is continuously condensing in the immediate surroundings of the S Dor star (Andriesse et al. 1978), and that the consensation process would produce a depletion of the heavier elements in the ejecta. (We assume that the X–rays are emitted farther out the dust condensation region). The stellar wind itself could have a "normal" iron abundance in line with the recent results of Hillier et al. (2001) who, from a non–LTE model fitting of the STIS/HST spectrum of η Car's central core (0.1 arcsec), found that the iron abundance in the stellar wind is roughly solar. However, their admitted uncertainty of a of factor two may well include the above–discussed iron underabundances. At any rate, the metal abundance in the optical and X–ray spectrum of η Car is an important problem that warrants future studies on new high quality data.

Let us finally consider the physical conditions required to produce the hot plasmas. If we base our analysis on the colliding–wind model, the temperatures of the shock waves formed in the collision region are related to the velocities of the stellar winds as they enter the shock (see e.g., Usov 1992). As discussed by Ishibashi et al. (1999) the 4.7 keV hard X–ray component of η Car implies a gas velocity of $\approx 1300/\mu^{1/2}$ km s^{-1}, where μ is the mean mass per particle. This velocity is definitely higher than the η Car maximum wind velocity of -800 km s^{-1} as derived from the blue edges of the UV resonance lines (Viotti et al. 1989). These lines are thought to be formed in the wind of the brighter S Dor component. If this velocity is taken as the wind terminal velocity, according to Usov's model it cannot provide the 4.7 keV plasma, and one comes to the conclusion that the hot plasma should be identified with the shocked wave produced by the high velocity wind of the O–type component of the system (Ishibashi et al. 1999).

Actually, observations have shown that η Car is ejecting matter at even higher velocities. As for instance, recently Weis et al. (1999) measured tangential motions of up to 1000 km s^{-1} in some filaments of the homunculus, corresponding to maximum radial velocities of about 2000 km s^{-1}. High velocity absorption components were identified in the Si IV 139.4 nm line (-1240 km s^{-1}, Viotti et al. 1989), and, as discussed above, in the

He I 1.083 μm line. In particular, it is worth noticing that the He I -1050 km s^{-1} absorption component is present in many spectra taken in different spectroscopic states of η Car. Since these high velocities have to be attributed to the S Dor component of the system, we cannot exclude that the terminal velocity of its wind could be higher than that derived from the blue edges of the UV resonance lines, and be high enough to produce the 4.7 keV shock wave.

As for the unseen component of the binary system, presumably it is an early–type supergiant. Then we expect this star to have a wind terminal velocity of 2000–3000 km s^{-1} (e.g., Kudritzky & Puls 2000). A terminal velocity of $\sim$1300 km s^{-1} seems to be more appropriate for a B0–0.5 supergiant star. Hence the hotter plasma responsible for the high energy tail might be associated with the shocked plasma facing the early–type stellar companion. This interpretation appears to be tentative, since at the moment it is not supported enough by the observations. In particular, we are completely lacking knowledge about the nature of the early–type star, nor there is any observational feature that could be undisputedly associated with its wind.

An important element could be knowing whether and how the source temperature is varying with the orbital phase. In fact, we know that the orbit of the η Car system should be very elliptical. Hence, we should expect that when near periastron the two stars approach, the velocity of the stellar wind(s) at the colliding zone could be slower than the terminal velocity, either because the wind has not yet reached the maximum velocity, or it is decelerated by the radiation of the other star (e.g., Usov 1992; Gayley et al. 1997). This effect, if present, would largely reduce the shock temperature, since as known, the temperature varies as the square of the gas velocity.

The ASCA and BeppoSAX observations show that the temperature of the 4.7 keV X–ray component is constant within the errors, possibly except near the spectroscopic minimum, while the behaviour of the temperature of the hotter source with the orbital phase is unknown. Actually, we do not know even whether the latter is thermal emission, and if it is located in a region different from that of the colliding wind.

5. Conclusion

The BeppoSAX observations described in this paper have shown some new aspects of the X–ray spectrum of η Car. In particular:

We have for the first time identified in December 1996, during the η Car's high state, a high energy ($E > 10$ keV) tail in marked excess with respect to the extrapolated 4.7 keV bremsstrahlung component. This result indicates that the modelling of the "core" X–ray emission of η Car requires a multi–temperature model, or alternatively, a nonthermal model.

In the X–ray emitting region iron could be underabundant, a result that may have an interesting link with the problem of the continuous dust condensation in η Car's

wind. At any rate, the important problem of the metal abundance in the optical and X–ray spectrum remains open and awaits further studies.

The comparison of the March 1998 BeppoSAX observation with that of December 1996 and with the ASCA observation of December 1997 have shown that there was a time shift of a few to several weeks between the hard X–ray and optical emission line flux minimum and the maximum of the absorption column density $NH_{\rm h}$. This might suggest that they represent two distinct phenomena: the quencing of the high energy source(s) and the temporary appearence (or formation) of an opaque region of unknown geometry in front of the source.

The binary model is at the moment incapable in explaining the overall scenario that is obtained from the observations. In this regard, it will be crucial to study the multifrequency behaviour of η Car during the next spectroscopic low state in June 2003.

References

Altamore, A., Maillard, J.-P., & Viotti, R. 1994, A&A, 292, 208

Andriesse, C. D., Donn, B. D., & Viotti, R. 1978, MNRAS, 185, 771

Chlebowski, T., et al. 1984, ApJ, 281, 665

Corcoran, M. F., Rawley, G. L., Swank, J. H., & Petre, R. 1995, ApJ, 445, L121

Corcoran, M. F., Petre, R., Swank, J. H., et al. 1998, ApJ, 494, 381

Corcoran, M. F., Fredericks, A. C., Petre, R., Swank, J. H., & Drake, S. A. 2000, ApJ, 545, 420

Corcoran, M. F., Ishibashi, K., Swank, J. H., & Petre, R. 2001, ApJ, 547, 1034

Damineli, A. 1996, ApJ, 460, L49

Damineli Neto, A., Viotti, R., Baratta, G. B., & de Araujo, F. X. 1993, A&A, 268, 183

Damineli, A., Conti, P. S., & Lopes, D. F. 1997, New Astron., 2, 107

Damineli, A., Kaufer, A., Stahl, O., Lopes, D. F., & de Araujo, F. X. 2000, ApJ, 528, L101

Davidson, K., Dufour, R. J., Walborn, N. R., & Gull, T. R. 1986, ApJ, 305, 867

Davidson, K., Ishibashi, K., Gull, T. R., & Hymphreys, R. M. 1999, Proc. Conf. Eta Carinae at the Millennium, ed. J. A. Morse, R. Humphreys, & A. Damineli, ASP Conf. Ser., 179, 227

Davidson, K., Ishibashi, K., Gull, T. R., Humphreys, R. M., & Smith, N. 2000, ApJ, 530, L107

Eichler, D., & Usov, V. 1993, ApJ, 402, 271

Feast, M., Whitelock, P., & Marang, F. 2001, MNRAS, 322, 741

Gayley, K., Owocki, S. P., & Crammer, S. 1997, ApJ, 475, 786

Ishibashi, K., Corcoran, M. F., Davidson, K., et al. 1999, ApJ, 524, 983

Kudritzki, R.-P., & Puls, J. 2000, ARA&A, 38, 613

Mewe, R., Gronenschild, E. H. B. M., & van den Oord, G. H. J. 1985, A&AS, 62, 197

McGregor, P. J., Rathborne, J. M., & Humphreys, R. M. 1999, Proc. Conf. Eta Carinae at the Millennium, ed. J. A. Morse, R. Humphreys, & A. Damineli, ASP Conf. Ser., 179, 236

Molendi, S., De Grandi, S., & Fusco–Femiano, R. 2000, ApJ, 533, L43

Osterbroek, T., Parmar, A. N., Mereghetti, S., & Israel, G. L. 1998, A&A, 334, 925

Rodgers, A. W., & Searle, L. 1967, MNRAS, 135, 99

Tsuboi, Y., Koyama, K., Sakano, M., & Petre, R. 1997, PASJ, 49, 85

Usov, V. V. 1992, ApJ, 389, 635

Viotti, R. 1969, Proc. Liège Coll. Les Transitions Interdites dans les Spectres des Astres, 54, 333

Viotti, R., Rossi, L., Cassatella, A., & Altamore, A. 1989, ApJS, 71, 983

Viotti, R., Corcoran, M. F., Damineli, A., & Grandi, P. 1998, Proc. Symp. The Active X-Ray Sky, ed. L. Scarsi, et al., Nuclear Phys. B (Proc. Suppl.), 69/1-3, 36

Viotti, R., Grandi, P., Antonelli, A., Corcoran, M. F., & Damineli, A. 1999, Proc. Conf. Eta Carinae at the Millennium, ed. J. A. Morse, R. Humphreys, & A. Damineli, ASP Conf. Ser., 179, 275

Walder, R., Folini, D., & Motamen, S. M. 1999, Proc. IAU Symp., 193, Wolf-Rayet Phenomena in Massive Stars and Starburst Galaxies, ed. K. A. van der Hucht, G. Koenigsberger, & P. R. J. Eenens, Astr. Soc. Pacific, 298

Weis, K., Duschl, W. J., & Chu, Y.-H. 1999, A&A, 349, 467

White, S. M. 2001, update of White, S. M., Duncan, R. A., Lim, J., & Drake, S. A. 1997, ASP Conf. Ser., 120, 282, Updated at `http://www.astro.umd.edu/~white/images/eta_time_full.html`

Zanella, R., Wolf, B., & Stahl, O. 1984, A&A, 137, 79